NORSAR

ROYAL NORWEGIAN COUNCIL FOR SCIENTIFIC AND INDUSTRIAL RESEARCH

Scientific Report No. 2-85/86

SEMIANNUAL TECHNICAL SUMMARY

1 October 1985 – 31 March 1986

L.B. Loughran (ed.)

Kjeller, May 1986

VII. SUMMARY OF TECHNICAL REPORTS/PAPERS PREPARED

VII.1 Regional event detection using the NORESS array

Since January 1985 data from the small-aperture array NORESS in Norway have been processed in real time at the NORSAR data center at Kjeller. The data used in the detection processing comprise 25 SPZ channels, deployed over an area 3 km in aperture and sampled at a 40 Hz rate. The detection algorithm has been described by Mykkeltveit and Bungum (1984), and briefly consists of

- Digital narrow-band filtering (six filter)
- Beamforming (conventional and incoherent)
- STA/LTA detector applied to each beam
- Frequency-wavenumber analysis of detected signals
- Association of regional phases to aid in locating events.

Preliminary results from the NORESS processing have earlier been presented in NORSAR Semiannual Technical Summaries (SATS). In this paper, we discuss in particular the automatic detection performance for events at regional distances, and the spectral characteristics of signal and noise at very high frequencies.

Regional detectability

An assessment of the NORESS detection capability at regional distances has been obtained by comparing the automatic NORESS detector output to the bulletins produced on the basis of local seismic networks in Fennoscandia. In particular, we have used as a data base the catalogue of seismic events in Northern Europe regularly compiled at the University of Helsinki.

The time period covered by this study is the 6-month interval April-September 1985, during which the RONAPP processor was operated with a fixed beam deployment (re. NORSAR SATS 84-85). A total of 477 events reported in the Helsinki catalogue (Fig. VII.1.1a) with local magnitudes in the range 1.7-3.3, were cross-checked with the NORESS detection

list. The epicentral distances from NORESS ranged from 500 to 1500 km. For each event, the expected arrival times at NORESS for P, Sn and Lg were computed, using standard travel time tables, and matched to NORESS detection entries.

Fig. VII.1.1b shows the magnitude-distance distribution of the events in the data base. Events detected at NORESS are shown as crosses, non-detections are indicated as triangles. In this figure, "detection" means that at least one phase (P, Sn or Lg) was reported by NORESS.

A summary of the statistics on automatic detection of primary vs. secondary phases is given in Table VII.1.1. We note that, at low magnitudes, many events are detected only on secondary phases. It is also noteworthy that several events, even in the higher magnitude range, are detected as P-phases only. However, visual inspection of the signal traces shows that in virtually all of these cases an Lg phase may be identified by the analyst. Thus, the lack of secondary phase detections is a problem within the automatic processor that requires improvements in the algorithms in order to extract emergent phases in the coda of a preceding P-phase.

M_L	1.5-2.0	2.1-2.5	2.6-3.0	3.1-3.5
P detection only	13	39	16	0
P + secondary phase*	16	105	30	3
Secondary phase only*	28	88	2	0
No detection	48	87	2	0
Total	105	319	50	3

* "Secondary phase" meaning Sn or Lg (or both) detected.

Table VII.1.1 Summary of automatic NORESS detection statistics for the regional data base.

Fig. VII.1.1 shows that there is only a slight degradation in detection capability with increasing distance for the range considered. As an initial estimate of detection thresholds, we have therefore combined the data in the distance range 700-1400 km and estimated detection thresholds as shown in Fig. VII.1.2 (detection on either P, Sn or Lg) and Fig. VII.1.3 (P-detection only). The method described by Ringdal (1975) has been applied.

From Fig. VII.1.2 we observe that the 50 and 90 per cent regional detection thresholds are close to M_L = 1.9 and 2.5, respectively. When only P phase detections are counted (Fig. VII.1.3), the respective thresholds are M_L = 2.3 and 2.7.

It would clearly be desirable to tie these thresholds to the global m_b scale. It has, however, not been possible to do this for the present data set, since all of the 477 reference events are much too small to have any teleseismic detection. Nevertheless, the local magnitude scale in question has been developed so as to be consistent with world-wide m_b, and the differences are not thought to be significant. This topic will be subject to further study.

As a final note, we remark that the large majority of reference events are mining explosions, mostly from mines in Western Russia. We have not yet attempted systematically to compare the detectability of these explosions to that of the (very few) earthquakes in the data base, but initial studies do not indicate major differences for the two source types.

High-frequency studies

The recently installed high-frequency recording system (HFSE) at NORESS has provided a unique opportunity to study noise and signal characteristics at frequencies up to at least 50 Hz. These studies

have only begun, but it is already apparent that much important information can be extracted from the high frequency part of the spectrum.

An example of a high-frequency recording is shown in Fig. VII.1.4, corresponding to an M_L = 5.0 earthquake off the west coast of Norway on February 6, 1986 (distance = 417 km). The unfiltered record shows the expected amplitude pattern, i.e., Lg as the dominant phase, Pg much larger than Pn. The picture changes dramatically when considering the high-frequency part of the record. In the filter band 30-50 Hz, the Pn and Sn phases dominate the seismogram, and the Pg and Lg phases are not even visible.

Fig. VII.1.5 shows HFSE spectra from the vertical component for the same event. We see that Lg exceeds the preceding noise (which in fact is the Sn coda) only up to about 10 Hz, whereas Pn has large SNR over the entire frequency band.

A further discussion of recorded HFSE P-wave spectra at various distances is given in Subsection VII.2.

In conclusion, the NORESS regional detection capability appears to be M_L = 2.5 or better out to at least 1500 km. Many small events are detected only on secondary phases, and the further improvement of automatic detection of such phases is important. At distances up to 500 km, considerable improvements in detection capability are possible by taking advantage of the high frequencies which propagate very efficiently in this distance range. The high frequency band is also potentially valuable for improved phase identification, especially to separate Pn from Pg and Sn from Lg.

F. Ringdal

References

Loughran, L.B. (ed.) (1985): NORSAR Semiannual Technical Summary, 1 Oct 84-31 Mar 85.

Loughran, L.B. (ed.) (1985): NORSAR Semiannual Technical Summary, 1 Apr - 30 Sep 1985.

Mykkeltveit, S. & H. Bungum (1984): Processing of regional seismic events using data from small-aperture arrays, BSSA, 74, 2313-2333.

Ringdal, F. (1975): On the estimation of seismic detection thresholds, BSSA, 65, 1631-1642.

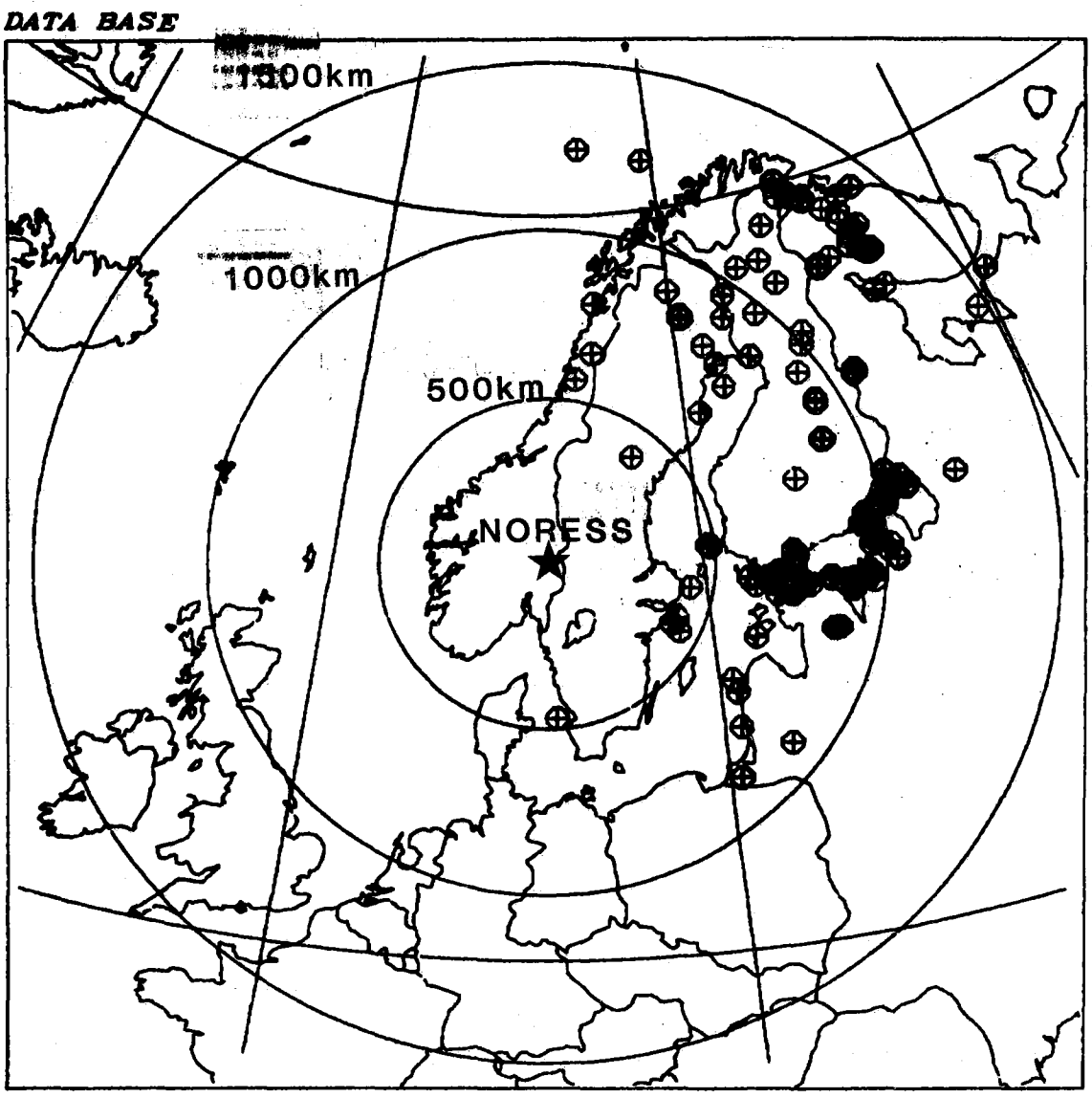

Fig. VII.1.1a Geographical distribution of 477 reference events used as a data base for the detectability study in this paper.

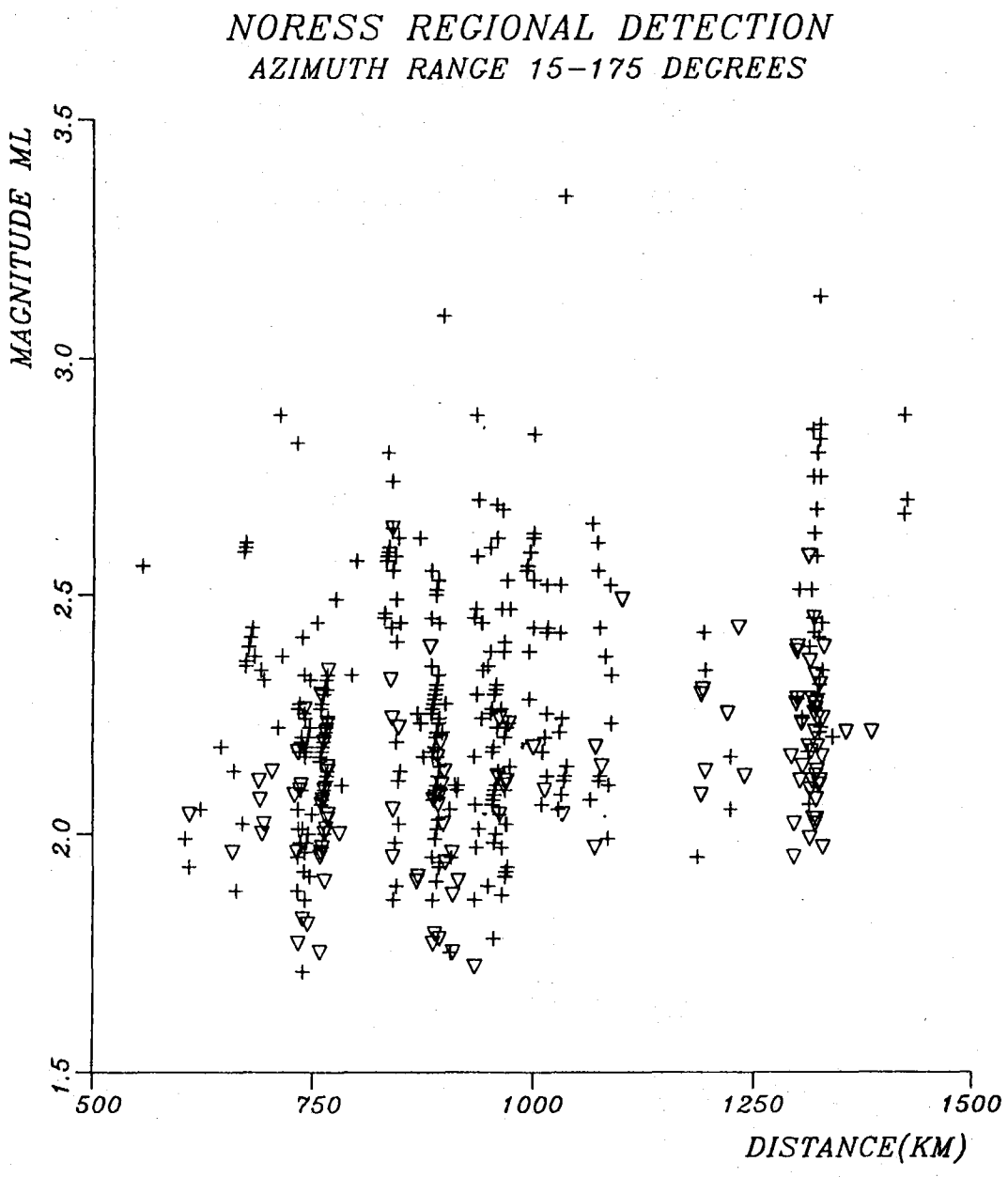

Fig. VII.1.1b Distribution of events in the data base as a function of epicentral distance from NORESS and local magnitude M_L. Crosses denote events detected automatically at NORESS (either P, Sn or Lg phase), whereas non-detected events are marked as triangles.

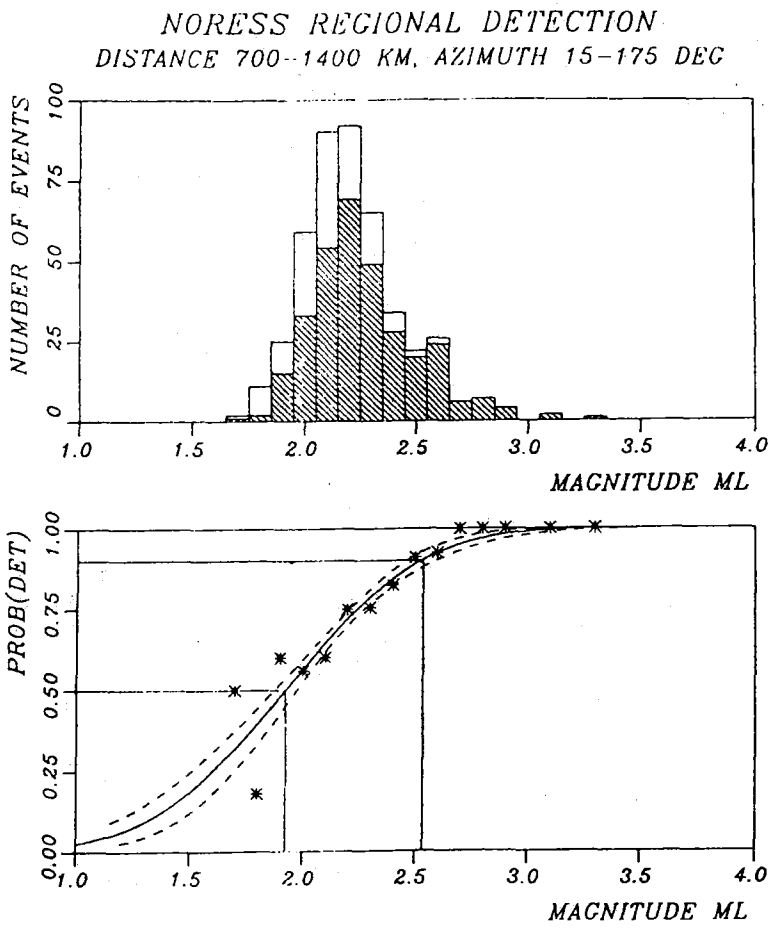

Fig. VII.1.2 Distribution of events by magnitude (upper part), with events detected for at least one phase (P, Sn or Lg) corresponding to the hatched columns. The bottom part of the figure shows the estimated detection probability curve as a function of magnitude, with the observed detection percentages marked as asterisks.

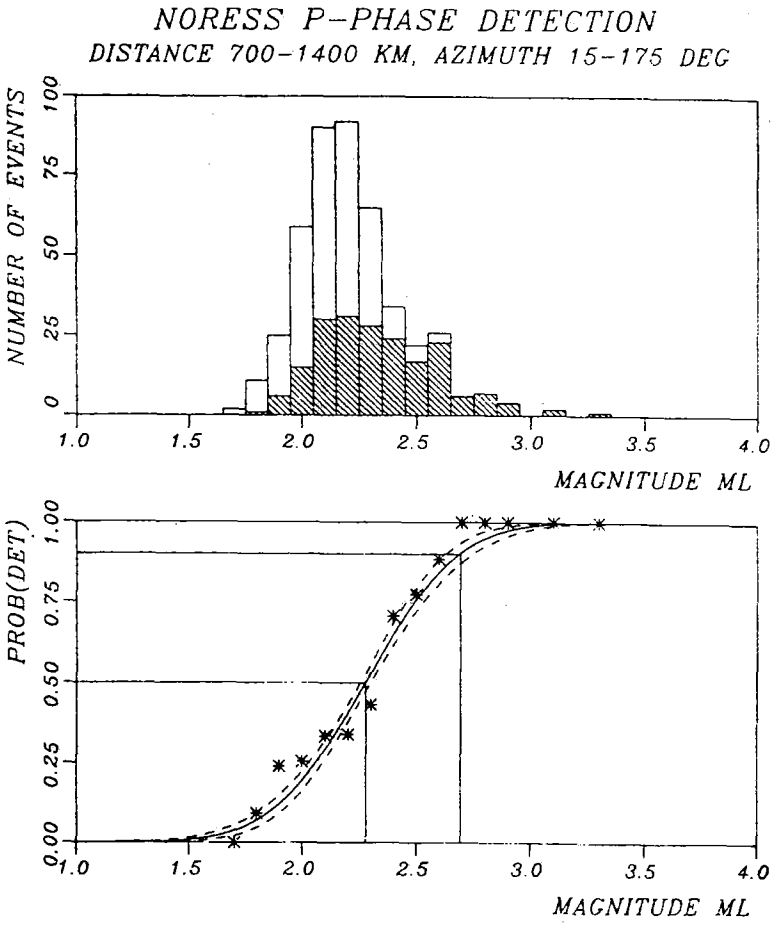

Fig. VII.1.3 Same as Fig. VII.1.2, except that only events with a detected P-phase are counted as detections.

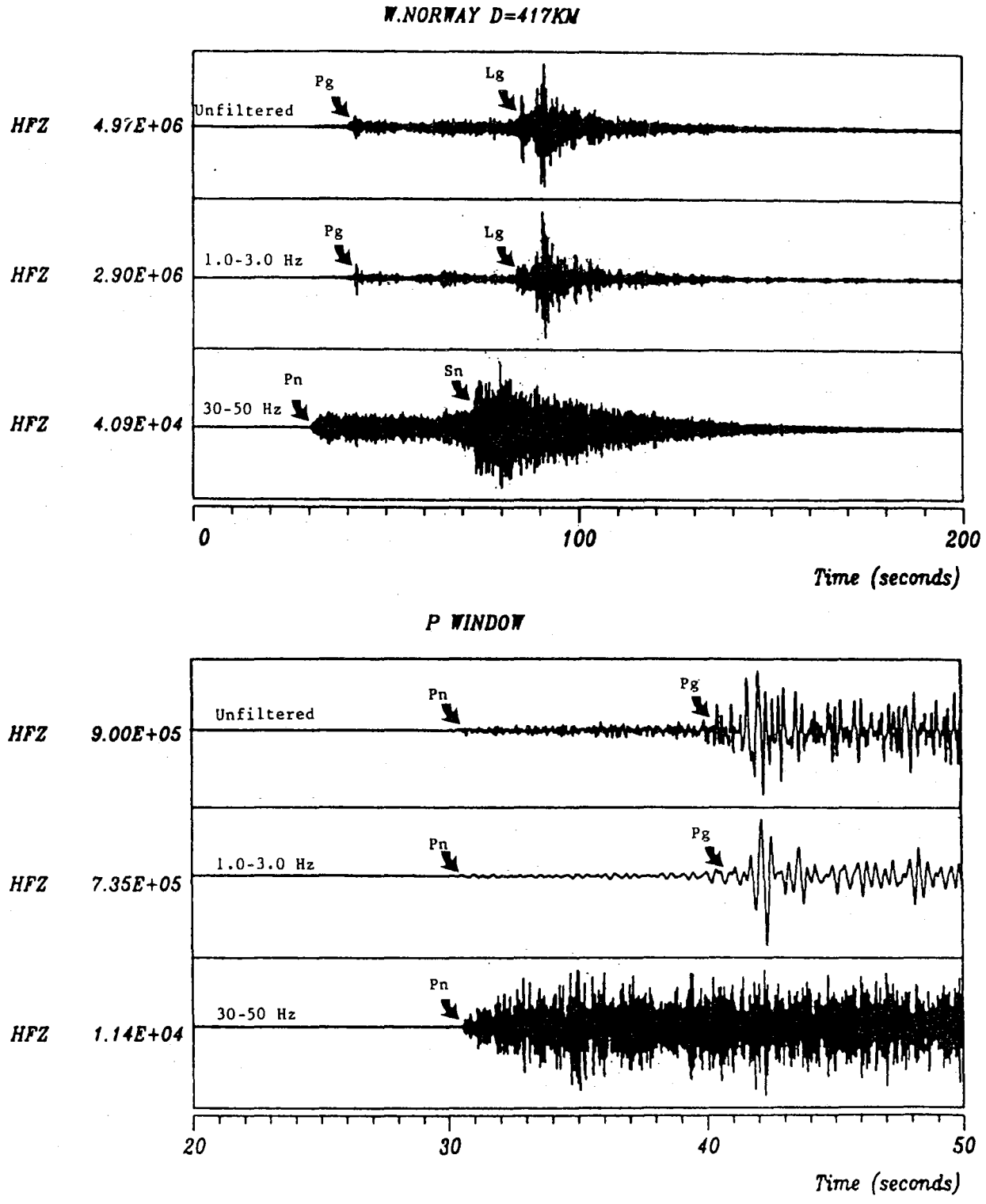

Fig. VII.1.4 Time domain plots of the HFSE recordings on the SPZ channel at NORESS for an M_L = 5.0 earthquake off the west coast of Norway (distance = 417 km). The upper part covers the entire wavetrain (unfiltered and in two filter bands as indicated). The bottom part is an expanded view of the P window. Note the prominence of Pn and Sn in the high-frequency band.

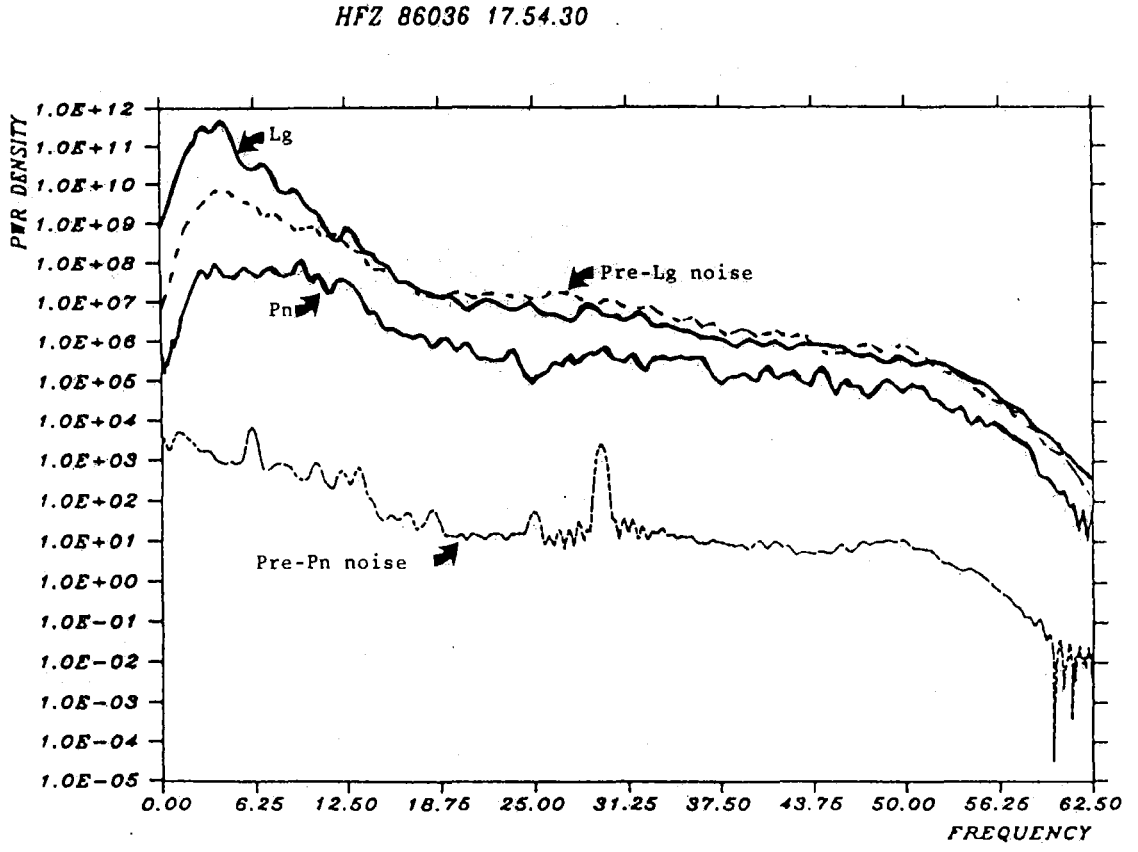

Fig. VII.1.5 Spectral plot of the Pn and Lg phases for the event shown in Fig. VII.1.4. Note that the Pn SNR remains approximately constant across the entire high-frequency part of the spectrum.